PROCEEDINGS OF SCIENCE

Recursive box and vertex integrations for the one-loop hexagon reduction in the physical region

Elise de Doncker*
Western Michigan University
E-mail: elise.dedoncker@wmich.edu

Junpei Fujimoto
High Energy Accelerator Research Organization (KEK)
E-mail: junpei.fujimoto@kek.jp

Nobuyuki Hamaguchi
Hitachi, Ltd., Software Division
E-mail: nobuyuki.hamaguchi.xr@hitachi.com

Tadahi Ishikawa
High Energy Accelerator Research Organization (KEK)
E-mail: tadashi.ishikawa@kek.jp

Yoshimasa Kurihara
High Energy Accelerator Research Organization (KEK)
E-mail: yoshimasa.kurihara@kek.jp

Yoshimitsu Shimizu
High Energy Accelerator Research Organization (KEK)
E-mail: yohimitsu.shimizu@kek.jp

Fukuko Yuasa
High Energy Accelerator Research Organization (KEK)
E-mail: fukuko.yuasa@kek.jp

We provide a technique which makes an efficient numerical evaluation feasible for the n-dimensional triangle functions and $n+2$-dimensional box functions, resulting from a reduction of the one-loop hexagon integral. At the level of the three- and four-point functions, a dimensional recursion of an adaptive numerical integration with extrapolation is effective for the corresponding low-dimensional integrals, even to integrate through threshold singularities present in cases of physical kinematics. An important reason for the reduction to these levels (in lieu of resorting to analytical formulas at a higher level), is that infrared divergences are made transparent so they can be separated. We give results for various sets of kinematic configurations, showing the feasibility and accuracy of the approach. Thus a bridge is provided between the computations of the reduction and direct numerical integration at a lower level.

13th International Workshop on Advanced Computing and Analysis Techniques in Physics Research
February 22-27, 2010
Jaipur, India

*Speaker.

PoS(ACAT2010)073

1. Introduction

The one-loop n-dimensional hexagon function can be reduced into (a linear combination of) $n+2$-dimensional box functions and n-dimensional triangle functions at the lowest level. A reduction to this level is preferred to, e.g., an analytic evaluation at a higher level as it uncovers and allows separating terms arising due to possible IR divergence. The basic n-dimensional triangle and box functions are expressed as two- and three-dimensional integrals, respectively [6].

For physical kinematics, the integrand functions may depict non-integrable singularities through vanishing denominators, but the expression has physical meaning by considering the function in the complex plane and taking the limit of the integral as a parameter approaches zero. In this paper we give a numerical approach by *(i)* addressing the limit via convergence acceleration (extrapolation) of a sequence of integrals; and *(ii)* approximating each integral in the sequence by a one-dimensional adaptive integration applied recursively in each integration direction. We refer to the latter as *dimensional recursion*. In general, the integrals of the sequence in *(ii)* have integrable singularities for physical kinematics and can be targeted by an adaptive domain partitioning.

We illustrate the numerical procedure by a simple example, for $\lim_{\alpha\to 0}\int_0^1 dx_1\int_0^1 dx_2\, I(\alpha)f$ where

$$I(\alpha)f \;=\; \int_0^1 dx_1\int_0^1 dx_2\,\frac{2\alpha x_2}{(x_1+x_2-1)^2+\alpha^2} \;=\; 2\arctan\frac{1}{\alpha}-\alpha\log(1+\frac{1}{\alpha^2}). \tag{1.1}$$

Table 1 lists integral approximations $Q(\alpha)f$ for $\alpha = 10^{-p}$, $p = 0,1,\ldots,7$. The values in the second column are obtained by dimensional recursion of the integration code DQAGE from the QUADPACK [10] package, with corresponding *absolute error* $|Qf - If|$ and the *number of integrand evaluations* (as a measure of the computational effort) for the integral approximation in columns 6 and 7, respectively.

The dimensional recursion adaptive procedure works well for this problem, where the integrand has a ridge at $x_1+x_2-1=0$, which becomes steeper with decreasing α. The procedure is justified in [9] and an error strategy is given in [7]. For comparison, the absolute error and number of evaluations for the standard adaptive multivariate integration code DCUHRE [1] are given in the last two columns [7]. The maximum number of evaluations was set to 100 million and the performance of DCUHRE breaks down for $p \geq 5$.

The columns in Table 1 under *Extrapolation* are obtained by convergence acceleration of the first column using the ε-algorithm [11]. The convergence (to π) improves in successive columns.

p	$Q(10^{-p})f$	Extrapolation	DQAGE × DQAGE		DCUHRE	
			ABS. ERR.	# EVAL.	ABS. ERR.	# EVAL.
0	0.877649149		1.11e-16	225	1.24e-12	3843
1	2.480743286	3.315088757	0.00e+00	21255	2.06e-12	144165
2	**3**.029488916	3.146268404 3.141547464	2.40e-13	93135	5.96e-12	199867
3	**3.1**25777143	3.141849664 3.141592605 3.141592651	3.49e-13	208035	1.37e-12	21040551
4	**3.1**39550588	3.141610354 3.141592651 **3.14159265**7	1.58e-13	388125	8.04e-12	99999963
5	**3.141**342396	3.141594001 **3.14159265**6	4.49e-13	561585	4.40e-07	99999963
6	**3.1415**63021	**3.141592**765	4.49e-13	561585	4.40e-07	99999963
7	**3.1415**89231		1.42e-10	686745	1.99e+00	99999963

Table 1: Sample problem: dimensional recursion and extrapolation

For $p \geq 2$, a new lower diagonal is added to the triangular extrapolation table.

The validity of the extrapolation procedure depends on the asymptotic behavior of the given sequence as $\alpha \to 0$. Note that (1.1) can be expanded using $\arctan \frac{1}{\alpha} = \pi/2 - \alpha + \alpha^3/3 - \alpha^5/5 + \ldots$, $|\alpha < 1|$. Knowledge of the expansion justifies linear extrapolation methods in this case. The ε-algorithm is known to be valid for an underlying expansion with terms of the general forms α^ν and $\alpha^\nu \log^k(\alpha)$, with real ν and $k \geq 0$ integer.

With respect to subsequent sections, an overview of the reduction procedure for the loop integrals is given in Section 2. Section 3 presents our numerical evaluation of the triangle and box building blocks and results are given in Section 4.

2. Reduction of n-dimensional N-point function

We consider a representation of the n-dimensional N-point function given by

$$I_N^n = (-1)^N \Gamma(N - n/2) \int_0^\infty \delta(1 - \sum_{j=1}^N x_j) \, \frac{\mathscr{U}^{N-n}}{\mathscr{F}^{N-n/2}} \tag{2.1}$$

where the functions $\mathscr{U}$ and $\mathscr{F}$ are determined by the momentum representation of the corresponding graph. Through the reduction formalism applied in [4, 6], the n-dimensional hexagon, pentagon and box functions are expressed in terms of n-dimensional triangle and $n+2$-dimensional box functions.

In non-exceptional kinematic conditions where the leading singularity of the N-point function [8] is not probed, the reduction is based on

$$I_N^n = \sum_{k=1}^N B_k I_{N-1,k} + (N - n - 1) \, \frac{\det(G)}{\det(S)} \, I_N^{n+2}, \tag{2.2}$$

$\det(S) \neq 0$, where G is the Gram matrix, $G_{k\ell} = -(r_\ell - r_k)^2$, with $r_\ell = \sum_{j=1}^\ell p_j$ and p_j are the external momenta; furthermore $S_{k\ell} = -(r_\ell - r_k)^2 + m_\ell^2 + m_k^2$, $1 \leq k, \ell \leq N$.

The reduction coefficients are defined as

$$B_k = -\sum_{\ell=1}^N S_{k\ell}^{-1}, \tag{2.3}$$

and can be obtained by solving the system of linear equations $\sum_{\ell=1}^N S_{k\ell} B_\ell = -1$, $k = 1, \ldots, N$.

In view of $\mathrm{rank}(S) = \min\{6, N\}$, it follows that $\det(S) = 0$ for $N > 6$. In cases where the matrix S is singular, the matrix inverse in the representation of the reduction coefficients can be replaced by its pseudo-inverse [3]. Furthermore, in non-exceptional kinematic conditions, N-point functions with $N \geq 6$ can be expressed in terms of pentagon functions since $\mathrm{rank}(G) = \min\{4, N-1\}$.

The reduction of the n-dimensional hexagon function results in:

hexagon I_6^n = a linear combination of six pentagon I_5^n functions;
pentagon I_5^n = a linear combination of five box I_4^n functions $+ \mathscr{O}(4-n)$;
box I_4^n = a linear combination of four triangle I_3^n functions and a box I_4^{n+2} function.

In order to account for IR divergence where $n = 4 - 2\varepsilon$, the $\mathscr{O}$ term in the pentagon reduction vanishes in the limit as $n \to 4$.

Thus we are left with the computation of a set of triangle functions I_3^n and box functions $I_4^{\hat{n}}$ with $\hat{n} = n+2$. According to the topology of the one-loop graph, the numerator of (2.1) is $\mathscr{U}(x) = \sum_{j=1}^N x_j$, since each chord through a single cut of the loop gives rise to a degree-1 monomial x_j, and $\mathscr{U}$ corresponds to the sum of these monomials (see, e.g., [5]). The denominator is

$$\mathscr{F}(x) = \hat{\mathscr{F}}(x) + \mathscr{U}(x) \sum_{j=1}^N x_j m_j^2, \tag{2.4}$$

where $\hat{\mathscr{F}}(x)$ is defined in terms of the Mandelstam variables $s_j = p_j^2$ and $s_{ij\ldots} = (p_i + p_j + \ldots)^2$.

For the functions $I_3^n(s_1, s_2, s_3, m_1^2, m_2^2, m_3^2)$ and $I_4^{\hat{n}}(s_{12}, s_{23}, s_1, s_2, s_3, s_4, m_1^2, m_2^2, m_3^2, m_4^2)$, define the kinematic matrices

$$\hat{S}^{(3)} = \begin{pmatrix} 0 & s_2 & s_1 \\ s_2 & 0 & s_3 \\ s_1 & s_2 & 0 \end{pmatrix} \qquad \text{and} \qquad \hat{S}^{(4)} = \begin{pmatrix} 0 & s_2 & s_{23} & s_1 \\ s_2 & 0 & s_3 & s_{12} \\ s_{23} & s_3 & 0 & s_4 \\ s_1 & s_{12} & s_4 & 0 \end{pmatrix} \tag{2.5}$$

for $N = 3$ and $N = 4$, respectively, and let $S = \hat{S} + M$, $M_{k\ell} = m_k^2 + m_\ell^2$, for $k, \ell = 1, \ldots, N$; then

$$\hat{\mathscr{F}}(x) = x^\tau \hat{S} x/2, \quad \text{and} \quad \mathscr{F}(x) = x^\tau S x/2$$

and I_3^n and $I_4^{\hat{n}}$ follow from (2.1) and (2.4) with denominators

$$\mathscr{F}_{Tri} = (-s_1)x_3x_1 + (-s_2)x_1x_2 + (-s_3)x_2x_3 + (x_1 + x_2 + x_3) \sum_{j=1}^3 x_j m_j^2 - i\delta$$

and

$$\begin{aligned} \mathscr{F}_{Box} = \quad & (-s_{12})x_4x_2 + (-s_{23})x_1x_3 + (-s_1)x_4x_1 + (-s_2)x_1x_2 + (-s3)x_2x_3 + (-s_4)x_3x_4 \\ & + (x_1 + x_2 + x_3 + x_4) \textstyle\sum_{j=1}^4 x_j m_j^2 - i\delta. \end{aligned}$$

The reduction follows (2.2) for $N \geq 4$, with S determined via $\hat{S}^{(4)}$ in (2.5) and $\det(G) = -(B_1 + B_2 + B_3 + B_4)\det(S)$.

3. Recursive Integration for Triangle and Box Functions

3.1 Triangle functions

For an evaluation of I_3^n, the δ-function can be removed in favor of one of the variables, e.g., by setting $x_3 = 1 - x_1 - x_2$ and taking the integral over the unit triangle $x_1 + x_2 \leq 1$, $x_1 \geq 0, x_2 \geq 0$. The resulting integrand function may have a vanishing denominator. Apart from a possible IR singularity at $x_1 = x_2 = 0$, e.g., with $m_3 = 0$, the quadratic denominator my be zero within the integration region.

The IR singularity can be separated from the integral as in [6] through sector decomposition and expansion of the integrand in the resulting sector functions. Furthermore, successive sector

decompositions can be applied to separate overlapping singularities. In the following we apply one level of sector decomposition, which eliminates the δ-function in the integrand of (2.1) in a symmetric way.

I_3^n is split into three sector functions,

$$I_3^n(s_1,s_2,s_3,m_1^2,m_2^2,m_3^2) = -\Gamma(3-n/2) \sum_{\mathscr{P}_{(1,2,3)}} S_{Tri}^n(s_2,s_3,s_1,m_2^2,m_3^2,m_1^2) \tag{3.1}$$

where $\mathscr{P}_{(1,2,3)}$ is the set of cyclic permutations of $(1,2,3)$.

The IR divergent case is treated in depth in [6]. We focus on the numerical evaluation of the basic integrals for $n=4$,

$$S_{Tri}^4(s_1,s_2,s_3,m_1^2,m_2^2,m_3^2) = \int_0^1 dt_1 dt_2 \; \frac{1}{1+t_1+t_2} \; \frac{1}{At_2^2+Bt_2+C-i\delta}, \tag{3.2}$$

where A is quadratic, B is linear and C constant in the integration variable t_1.

For the evaluation in [6], the inner integral (in t_2) is obtained analytically, and the outer integration (in t_1) is performed numerically with the QUADPACK program DQAGS [10]. Whilst the strategy of DQAGS handles a class of singularities at the end-points of the integration interval, it has no mechanism to handle singularities at arbitrary points in the interior of the integration interval, other than its adaptive subdivision process to narrow in on a singular spot. The analytic outer integrand of (3.2) generally has 1/square root and logarithmic singularities in the interior of the integration domain.

Even though the NUMERIC $\times$ ANALYTIC method of [6] works well in 2D, it does not for the box functions. In 3D they resort to a Monte Carlo integration in the vicinity of the singularity for the outer (2D) NUMERIC integration, combined with a multivariate adaptive method (of DCUHRE [2]). We propose a simple recursive procedure of a numerical integration in each coordinate direction, for which we use a general adaptive integration program, DQAGE from QUADPACK. We first illustrate the method for the 2D triangle integral, DQAGE$\times$DQAGE$f \approx I_1(I_2 f)$, where $f(t_1,t_2)$ is the integrand of (3.2).

Splitting the real and imaginary parts of the integrand and setting $D = At_2^2+Bt_2+C$ yields

$$S_{Tri}^4(s_1,s_2,s_3,m_1^2,m_2^2,m_3^2) = I_1[I_2 f] = \int_0^1 dt_1 \left[\int_0^1 dt_2 \; \frac{1}{1+t_1+t_2} \; \frac{D+i\delta}{(D^2+\delta^2)} \right]. \tag{3.3}$$

Figure 1 shows plots of $I_2 f(t_1,t_2)$ as a function of t_1, evaluated in the course of the outer DQAGE integration for $S_{Tri}^{n=4}(6,4,1,1,1,1)$ and $S_{Tri}^{n=4}(10,4,\frac{5}{2},1,1,1)$ with $\delta = 10^{-12}$ in (3.3). These match the analytic calculation of $I_2 f$ in [6] and demonstrate the ability of DQAGE to track the singular behavior adequately. Sample Fortran code for $I_2 f(t_1)$ is given in Figure 2. The top level routine of DQAGE is duplicated as DQAGEX and DQAGEY to simulate the recursive call in Fortran. The main program (not shown) calls DQAGEX for the computation of the outer integral $I_1(I_2 f(t_1))$.

3.2 Box functions

Sector decomposition of I_4^{n+2} delivers four sector integrals of the form S_{Box}^{n+2}. For $n=4$ this is

$$S_{Box}^6(s_{12},s_{23},s_1,s_2,s_3,s_4,m_1^2,m_2^2,m_3^2,m_4^2) = \int_0^1 dt_1 dt_2 dt_3 \frac{1}{(1+t_1+t_2+t_3)^2} \; \frac{1}{At_2^2+Bt_2+C-i\delta}. \tag{3.4}$$

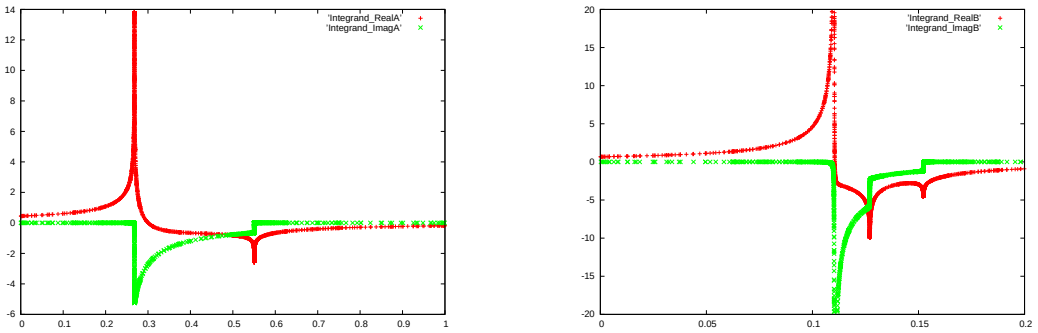

Figure 1: Numerical evaluation of *(Left:)* $S^4_{Tri}(6,4,1,1,1,1)$ and *(Right:)* $S^4_{Tri}(10,4,\frac{5}{2},1,1,1)$ by DQAGE

```
      double precision function fx(x)
      implicit real*8(a-h,o-z)
      parameter(nw = 1000)
      dimension alist(nw),blist(nw),elist(nw)
      dimension rlist(nw),iord(nw)
      common/wrk/epsa,epsr,lim,keyy
      common/limits/ay,by
      common/args/xx
      common/flags/iflagy
      external fy
      epsabs = epsa
      epsrel = epsr
      limit = lim
      xx = x
C Integration in y direction
      call Dqagey(fy,ay,by,epsabs,epsrel,keyy,limit,result,
     *     abserr,neval,ier,alist,list,rlist,elist,iord,last)
      if(ier.ne.0) iflagy = iflagy+1
      fx = result
      return
      end
```

```
      double precision function fy(y)
      implicit real*8(a-h,o-z)
      common/pars/del,sqdel,dm1,dm2,dm3,s1,s2,s3
      common/args/xx
      common/icnt/dkount
      dkount = dkount+1.d0
      aa = dm2
      bb = (dm1+dm2-s2)*xx+dm2+dm3-s3
      cc = dm1*xx*xx+(dm1+dm3-s1)*xx+dm3
      d = aa*y*y+bb*y+cc
      denom = d*d+sqdel
C Real part
C     fy = d/denom/(1+xx+y)
C Imaginary part
      fy = del/denom/(1+xx+y)
      return
      end
```

Figure 2: Sample program for numerical evaluation of $I_2 f(t_1,t_2)$

where A is constant, B is and C is a quadratic function in t_1 and t_2. In [6], the inner integral (in t_3) is evaluated analytically.

The analytic integrand has a complicated singularity structure. Apart from the fact that its implementation requires incorporating many different cases depending on the values of the parameters, the singularity renders the outer 2D integration problematic. The latter is performed in [6] using DCUHRE with a Monte Carlo integration in the vicinity of the singularity within the integration domain, where it is also mentioned that DCUHRE was used with a workspace limit of 350 MB to allow for a maximum of 1.5 10^9 2D function evaluations. Furthermore, the slow convergence rate of the MC integration is a problem.

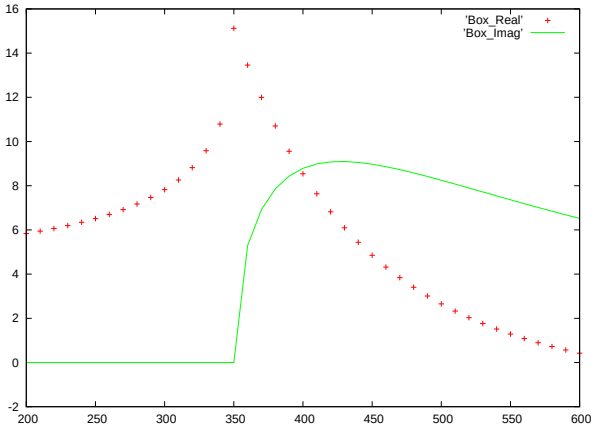

Figure 3: Threshold scan of 4-dimensional scalar box function

We find that we can efficiently compute the 3D integral recursively as a 1D×1D×1D integral, with DQAGE from QUADPACK [10] in each direction, without specifying the location or nature of the singularity.

4. Overview of results

We implemented the building block integrations (3.2) and (3.4) by dimensional recursion of the one-dimensional adaptive algorithm of DQAGE from QUADPACK [10]. In order to allow computations in the physical region, a sequence of integral approximations $Q(\delta)$ is computed for a geometric progression of δ with ratio $\frac{1}{2}$, for an extrapolation by the ε-algorithm [11]. We use a modification of the ε-algorithm code in QUADPACK. For each new integral $Q(\delta)$ in the original sequence, the new lower diagonal of the triangular ε-algorithm table is calculated and a new extrapolated value is returned.

The results in this paper are obtained for specified absolute error tolerances ε_a for the integrations. For all sample problems reported, the maximum number of subdivisions allowed in the adaptive partitioning process was fixed at 100 in each coordinate direction. The extrapolations were started at $\delta = 1$ and the maximum number of extrapolations was set to 20. The extrapolation process was terminated *normally* when the extrapolated sequence converged within $0.1\varepsilon_a$. All computations were run on a Macbook Pro laptop computer with 3.06 GHz Intel Core 2 Duo processor and 8 GB RAM.

As a test of the code for the 4-dimensional box function $I_4^{n=4}$, Figure 3 displays a scan of the $2m_t = 350$ GeV threshold of the box function from [6] with $s_{12} = (E_{cms}/(2m_t))^2$, $s_{23} = -(m_Z/(2m_t))^2/2$, $s_1 = s_2 = (m_Z/(2m_t))^2$, $s_3 = s_4 = (m_b/(2m_t))^2$, $m_1^2 = m_2^2 = m_4^2 = 1/4$, $m_3^2 = (m_W/(2m_t))^2$ and $m_t = m_{top} = 175$ GeV, $m_Z = 90$ GeV, $m_b = 5$ GeV, $m_W = 80$ GeV.

Other results are displayed in Table 2, for the Mandelstam variables listed in the first column. The symmetric (I) and modified symmetric parameters (II) correspond to Euclidean points. The

$\hat{\mathbf{S}}$	**Symmetric**					**Symmetric-mod**		**Physical kinematics**	
	$\mathbf{I}_3^n$	$\mathbf{I}_4^{n+2}$	$\mathbf{I}_4^n$	$\mathbf{I}_5^n$ (I)	$\mathbf{I}_6^n$ (I)	$\mathbf{I}_5^n$ (II)	$\mathbf{I}_6^n$ (II)	$\mathbf{I}_5^n$ (III)	$\mathbf{I}_6^n$ (III)
$\mathbf{s_{12}}$		-1	-1	-1	-1	-1	-1	4	4
$\mathbf{s_{23}}$		-1	-1	-1	-1	-1	-1	$-1/5$	$-1/5$
$\mathbf{s_{34}}$				-1	-1	-1	-1	$1/5$	$1/5$
$\mathbf{s_{45}}$				-1	-1	-1	-1	$3/10$	$2/5$
$\mathbf{s_{51}}$				-1		$-5/2$		$-1/2$	
$\mathbf{s_{56}}$					-1		-1		$3/10$
$\mathbf{s_{61}}$					-1		-1		$-1/10$
$\mathbf{s_{123}}$					-1		-1		$1/10$
$\mathbf{s_{234}}$					-1		-1		$-3/10$
$\mathbf{s_{345}}$					-1		$-5/2$		0.38189943
$\mathbf{s_1}$	-1	-1	-1	-1	-1	-1	-1	0	0
$\mathbf{s_2}$	-1	-1	-1	-1	-1	-1	-1	0	0
$\mathbf{s_3}$	-1	-1	-1	-1	-1	-1	-1	$49/256$	$9/100$
$\mathbf{s_4}$		-1	-1	-1	-1	-1	-1	$9/100$	$9/100$
$\mathbf{s_5}$				-1	-1	-1	-1	$49/256$	$9/100$
$\mathbf{s_6}$					-1		-1		$9/100$
$\mathbf{m_1^2}$	1	1	1	1	1	1	1	$49/256$	$49/256$
$\mathbf{m_2^2}$	1	1	1	1	1	1	1	$49/256$	$49/256$
$\mathbf{m_3^2}$	1	1	1	1	1	1	1	$81/1600$	$49/256$
$\mathbf{m_4^2}$		1	1	1	1	1	1	$81/1600$	$49/256$
$\mathbf{m_5^2}$				1	1	1	1	$49/256$	$49/256$
$\mathbf{m_6^2}$					1		1		$49/256$
	-0.40114016217730431	0.12843607593092609 7	0.09916512227141025	-0.03541611509693 22	0.01249980532832 90	-0.03203460837305 95	0.01352602689549 10	$\Re$e 41.34025332219 $\Im$m -45.9720825696	$\Re$e -26.933830586 $\Im$m 48.6351969959
Time 10^{-6}	0.00091	0.0176	0.0213	0.0972	0.586	0.0979	0.588	$\Re$e 132.8 $\Im$m 127.6	$\Re$e 361.7 $\Im$m 324.8
Time 10^{-9}	0.0034	0.0348	0.0485	0.228	1.370	0.258	1.493	$\Re$e 412.7 $\Im$m 421.9	$\Re$e 1395.2 $\Im$m 1455.0
Time 10^{-16}	0.0278	2.33	2.44	11.89	71.35	11.59	70.12		

Table 2: Overview of results

physical points (III) for the $n = 4$-dimensional pentagon and hexagon functions correspond to kinematic configurations arising in the processes $\gamma\gamma \to t\bar{t}H$ and $\gamma\gamma \to HHHH$, respectively. In addition to the masses listed above, $m_{Higgs} = 120$ GeV is used and all kinematic parameters are scaled by $E_{cms}/2 = 400$ GeV [6].

Results are given for high accuracy runs and match with the values given (to 4-digit accuracy) in [6]. User times (in CPU seconds, using the Fortran function *etime*) are shown for runs performed with requested integration accuracies of $\varepsilon_a = 10^{-6}, 10^{-9}$ and 10^{-16} (the latter for the Euclidean region). Note that the accuracies are specified as error tolerances for the basic integral computations, of which the errors will be combined in the linear combination of the n-point function.

It may be noted that, compared to a direct numerical computation at a higher level (e.g., the

level of the box integrals I_4^n given by (2.1)), the combined calculation of the lower level triangle (3.2) and box (3.4) integrals is far more accurate and less time-consuming.

Conclusions

We give an efficient and accurate approach for a numerical computation of the basic triangle and box functions resulting from a reduction of the one-loop hexagon function. Dimensional recursion of a one-dimensional adaptive integration algorithm is ideal for multivariate integrals in two or three dimensions where the integrand has some types of singularities in the interior of the integration domain.

We have shown that the approach is effective for various sets of configurations in the physical as well as the Euclidean region. This presents an interface between the higher level reductions and the lower level direct numerical integration, thereby alleviating detailed analytical formulations and their pitfalls associated with necessary knowledge of the location and structure of the singularity as well as possible cancellation errors.

References

[1] BERNTSEN, J., ESPELID, T. O., AND GENZ, A. An adaptive algorithm for the approximate calculation of multiple integrals. *ACM Trans. Math. Softw. 17* (1991), 437–451.

[2] BERNTSEN, J., ESPELID, T. O., AND GENZ, A. Algorithm 698: DCUHRE-an adaptive multidimensional integration routine for a vector of integrals. *ACM Trans. Math. Softw. 17* (1991), 452–456.

[3] BINOTH, T., GUILLET, J. P., AND HEINRICH, G. Reduction formalism for dimensionally regulated one-loop n-point integrals. *Nuclear Physics B572* (2000), 361. hep-ph/9911342v1.

[4] BINOTH, T., AND HEINRICH, G. An automized algorithm to compute infrared divergent multi-loop integrals. *Nuclear Physics B585* (2000), 741–759. hep-ph/0004013v2.

[5] BINOTH, T., AND HEINRICH, G. Numerical evaluation of multi-loop integrals by sector decomposition. *Nuclear Physics B680* (2004), 375–388. hep-ph/0305234v1.

[6] BINOTH, T., HEINRICH, G., AND KAUER, N. A numerical evaluation of the scalar hexagon integral in the physical region. *Nuclear Physics B654* (2003), 277–300. hep-ph/0210023v1.

[7] DE DONCKER, E., AND KAUGARS, K. Dimensional recursion for multivariate adaptive integration, 2010. Proceedings of the International Conference on Computational Science.

[8] EDEN, R. J., LANDSHOFF, P. V., OLIVE, D. I., AND POLKINGHORNE, J. C. *The Analytic S-Matrix*. Cambridge Univ. Press, 1966.

[9] LI, S. *Online Support for Multivariate Integration*. PhD dissertation, Western Michigan University, December 2005.

[10] PIESSENS, R., DE DONCKER, E., ÜBERHUBER, C. W., AND KAHANER, D. K. *QUADPACK, A Subroutine Package for Automatic Integration*. Springer Series in Computational Mathematics. Springer-Verlag, 1983.

[11] WYNN, P. On a device for computing the $e_m(s_n)$ transformation. *Mathematical Tables and Aids to Computing 10* (1956), 91–96.